Detailed Pseudo-Static Drive Train Modelling with Generator Short Circuit

Christopher Warnock, David Infield

CDT Wind Energy Systems, Rm 3.36 University of Strathclyde, 204 George Street, Glasgow, G1 1XW

Christopher.warnock@strath.ac.uk

Abstract. Drivetrain failures contribute significantly to wind turbine downtime. Although the root causes of these failures are not yet fully understood, transient events are regarded as an important contributory factor. Despite extensive drive train modelling, limited work has been carried out to assess the impact of a generator short circuit on the drivetrain. In most cases, a generator short circuit is classed as a failure in itself with minimal focus on the subsequent effects on the gearbox and other drivetrain components. This paper will look to analyse the loading on the drivetrain for a doubly fed induction generator (DFIG) short circuit event with turbine ride through using a combination of Simulink, Garrad Hassan's Bladed and RomaxWind drive train modelling software.

1. Background

As energy generation from offshore wind increases, it is essential that turbine downtime and maintenance costs are significantly reduced due to loss of generation resulting from limited access to turbines for repair. In depth analysis of wind turbine systems allows for efficient scheduling of maintenance, reduction of turbine downtime and optimisation of control strategies.

According to analysis carried out by Spinato and Tavner [1] using Windstats survey data, although the drivetrain, gearbox and generator's failure rates are lower than other failure modes such as electrical systems, the associated downtime is much greater as can be seen in Figure 1.

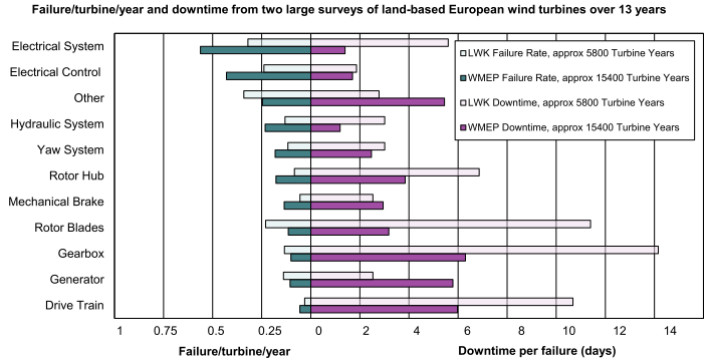

Figure 1: Reliability and downtime analysis of turbine subassemblies [1]

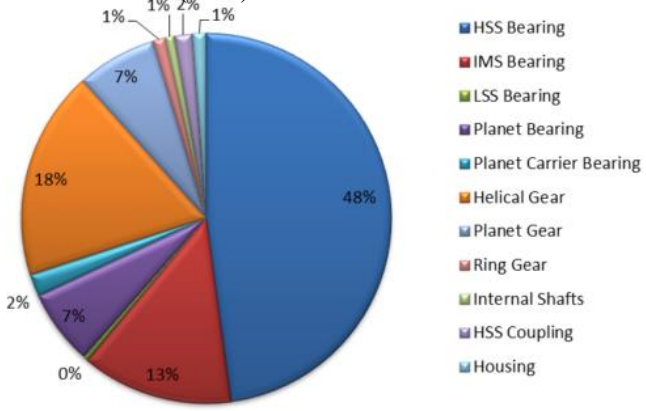

Figure 2: Component contribution to failure according to NREL gearbox failure database

Work carried out by Sheng with NREL has revealed the components within the drivetrain contributing most to failures. The High Speed Shaft (HSS) bearing accounts for 48% of failures from a database of 289 gearbox failure incidents. The data shows that both bearing and gear faults are concentrated in the parallel stage of the gearbox[2].

The DFIG is presently the most commonly used generator for wind turbines. Extensive modelling of DFIGs has been undertaken including analysis of short circuits to demonstrate ride through as required by grid codes. However, this research has focused in the main on the electrical aspects associated with the fault such as protection, the transient current contribution and local voltage impact, [3]–[5]. It should be noted that the most common cause of generator short circuit is a short within the power system network to which the generator is connected. Such events are not uncommon and this is the reason why grid codes require wind turbines to ride through such faults, thus minimizing adverse impacts on the network itself. Nevertheless such events will impose transient torque loads. Despite this, the subsequent mechanical loading on the drivetrain following a generator short circuit has not been adequately investigated in literature. An in depth analysis of the gearbox and drivetrain mechanics is presented here in order to identify which individual components are most affected by the resultant torque transient.

2. Methodology

2.1. Simulink Generator Model

The analysis involves using a combination of three models representing different stages of the drivetrain with varying degrees of fidelity. The generator has been represented by a 2MW DFIG model within Simulink. Primarily this model is used to investigate how protection and control can be implemented to mitigate the effects of generator faults however, in the context of this analysis it has been used to determine the transient torque profile transmitted to the High Speed Shaft (HSS). Using a wind speed of 10m/s so as to avoid controlled pitching during the event, a 3 phase short circuit has been simulated. According to grid code standards, a Generating Plant must be able to maintain grid connection during unbalanced and balanced faults for up to 140ms.[6] In this case a Generator Short Circuit (GSC) fault of 150ms has been used to simulate a wind turbine fault ride through.

.

The simulation has been carried out with and without crowbar protection enabled so as to assess the extent to which the crowbar can mitigate further loading on the drivetrain. In order to fully capture the effects of the GSC, a high sampling interval of 5e-5s (20 kHz) has been used.

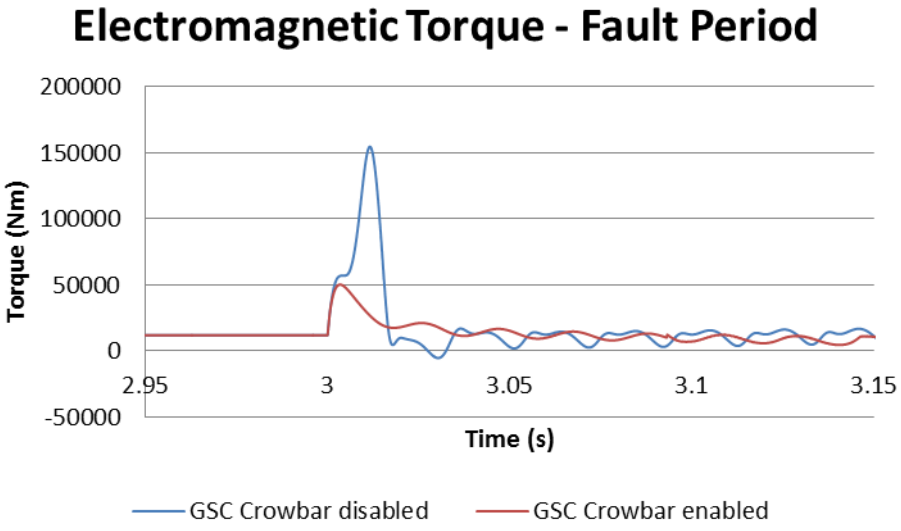

Figure 3: Resultant electromagnetic torque following a 3 phase short circuit with duration of 150ms

The fault has been triggered at 3seconds as shown in Figure 3. Directly following the short circuit, the electromagnetic torque spikes, followed by a torque reversal and continuing oscillations until the fault is cleared after 150ms. While it is clear that through enabling the crowbar protection the increase in torque has been significantly reduced as well as removing the initial torque reversal, the magnitude of this increase is almost fifteen times greater than that of steady state operational torque. This torque profile acts as the input parameters to a turbine model in Garrad Hassan's Bladed and represents the airgap torque produced by the generator as a result of the short circuit.

2.2. Bladed Turbine Model

The turbine model in Bladed represents a 2MW, 3 bladed upwind, variable speed turbine with a DFIG. Bladed uses a simplified model of a DFIG generator. However, when combined with this externally calculated torque profile it can simulate how the entire turbine will react following the GSC. Simulations have been carried out using both torque profiles to obtain the shaft rotational speeds and resultant Low Speed Shaft (LSS) torque under these conditions. Initially these were captured using a sample interval equal to that of the Simulink model of 5e-5 seconds. This was later reduced to 5e-3 seconds (200Hz) so as to reduce computational time while maintaining adequate resolution.

The torque profile has been applied to simulate a short circuit at 0.5s as opposed to 3s, again to minimise computational time. The generator torque shown in Figure 4 also shows a slightly different torque profile to that of the Simulink output. Figure 4 shows the torque observed at the generator during operation of the wind turbine and therefore includes all inertias within the drivetrain as opposed to the airgap torque profile produced by the generator without any consideration of inertia or other drive train properties. This has subsequently reduced the initial torque spike of the profile with the crowbar disabled. The fault is cleared at 0.65s and the turbine then begins to return to normal operation.

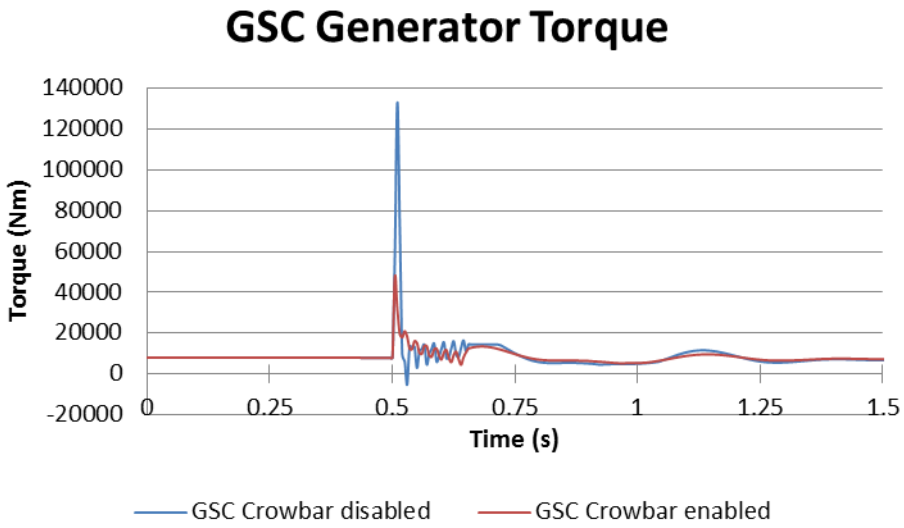

Figure 4: Generator torque obtained from Bladed simulation

Unlike the generator torque, the LSS torque shows a prolonged initial change in torque (Figure 5). In comparison to the reduction in torque provided by the crowbar in the generator torque, the effect on the LSS torque is not as significant. This is due to the limited energy associated with the torque spike observed in the generator torque. As the increase in torque occurred for such a short period, this has been absorbed by the inertias in the system including the generator inertia itself. As a result this profile is not reflected in the LSS torque. Upon clearing of the fault, the LSS torque moves towards normal operation however, due to the large inertia associated with the rotor and drive train torsional compliance, a torque reversal is at roughly 0.9s experienced. Loading reductions in the order of 600kNm can be seen throughout the fault and 300kNm on return to normal operation due to the crowbar thus showing that the crowbar can assist in reducing loading throughout the drivetrain as well as removing the torque reversal in the LSS.

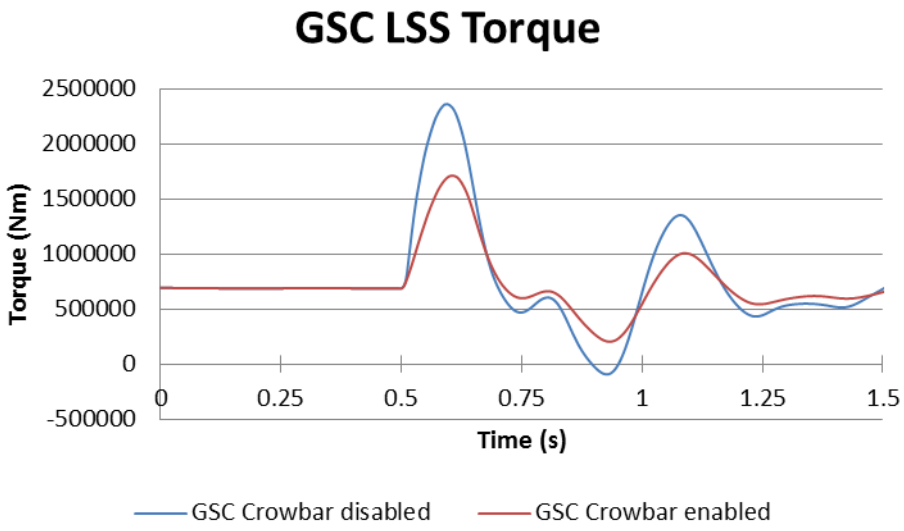

Figure 5: Low Speed Shaft torque obtained from Bladed model

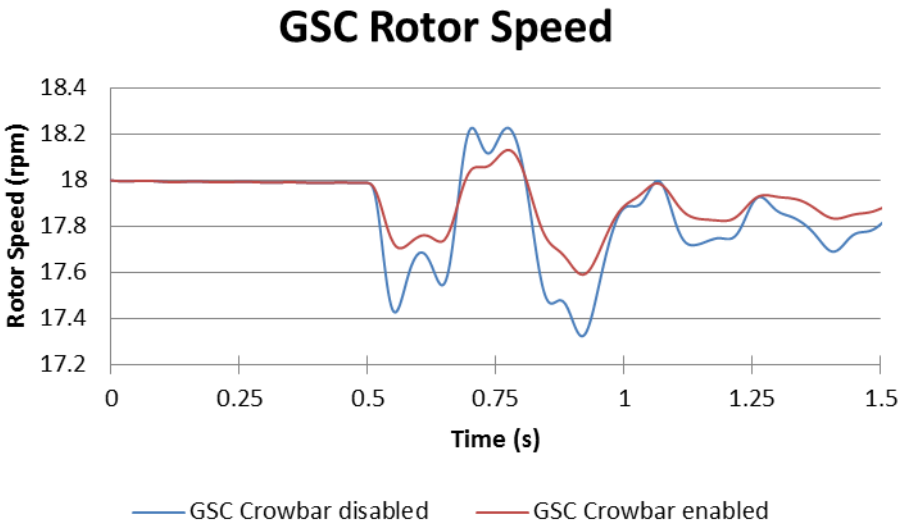

Figure 6: Rotor Speed obtained from Bladed model

The rotor speed of the turbine shows similar results where the effect of the short circuit is reduced by enabling the crowbar. It can also be seen that higher frequency variations observed with the crowbar disabled simulation are partially removed with the enabling of the crowbar.

2.3. RomaxWind Drivetrain Model

Much like the generator model within Bladed, the gearbox is represented by a simplified lumped mass model, which cannot provide insight into the effects experienced by the gearbox on a component level. In order to assess how the individual components react to this transient load, a detailed drivetrain model has been implemented in RomaxWind for which the time series calculated by Bladed act as the input parameters. Each 5e-3s time step provides a load case input to the RomaxWind model. These load cases are each run as a static model to provide a pseudo-static time domain model. Upon completion, the results are combined to provide a representation of the full transient event and its effects on the system. Work carried out by Kenneth Scott [7] compared the use of this pseudo-static approach to that of a fully dynamic model, showing that this method could sufficiently replicate the dynamic results.

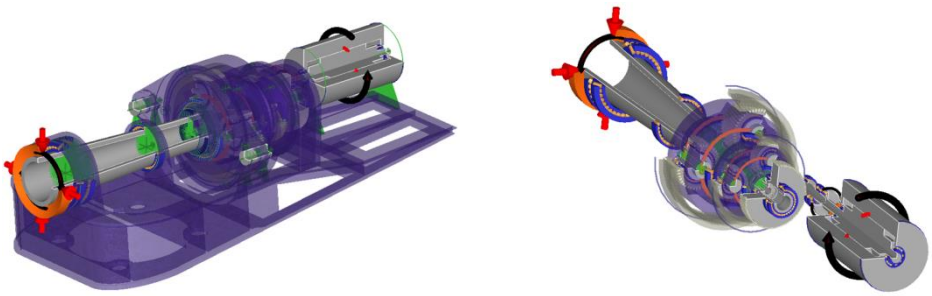

Figure 7: 2MW 3 stage drivetrain model in RomaxWind[7]

The drivetrain created in RomaxWind consists of a 2 stage planetary and 1 stage parallel gearbox along with LSS, HSS and generator. The model uses non-linear analysis to determine the deflections of shafts and non-linear contact to determine the loading on bearings and gears within the system. This analysis has investigated the housing displacement due to the GSC, the contact stresses experienced by

the gears and bearings and subsequently their associated safety factors. In order to place the effects of the GSC in context, a simulation of an Emergency Stop (Estop) has also been carried out alongside the crowbar enabled and disabled events.

3. RomaxWind Results

The modelling of the GSC event has been carried out using 3 duty cycles: the first of which focuses on the period of 0-0.495s, followed by 0.5-0.995 and 1-1.495s. Each of these contains 100 load cases, covering a simulation time of 1.5s. As shown in Figures 3-5, the short circuit is triggered at 0.5s and is cleared at 0.65s. In light of this, in some cases results have only been shown for the duty cycle encapsulating the short circuit event during the period of 0.5-0.995 as this period experienced the most significant loading.

3.1. Housing Displacement

Analysis of the gearbox housing focuses on the port and starboard pins used to connect the main gearbox housing to the bedplate. This is the primary point for supporting the gearbox and as such displays the gearbox movements with the greatest accuracy. These housing displacements can lead to bearing misalignment and subsequently additional damage to the bearings. The displacements outlined in Figure 7 represent the housing displacement in the Y-plane. During the steady state region of 0-0.495s there is no sign of displacement due to a constant torque being applied to the system (Figure 8). During the GSC at 0.5s the displacement of the housing mirrors the profile of the LSS torque shown in Figure 4, with the starboard pin initially starting in a positive position and moving to negative displacement. These oscillations continue until the end of the simulation where only the starboard pin with the crowbar disabled changes polarity as the oscillations diminish, returning to their steady state position.

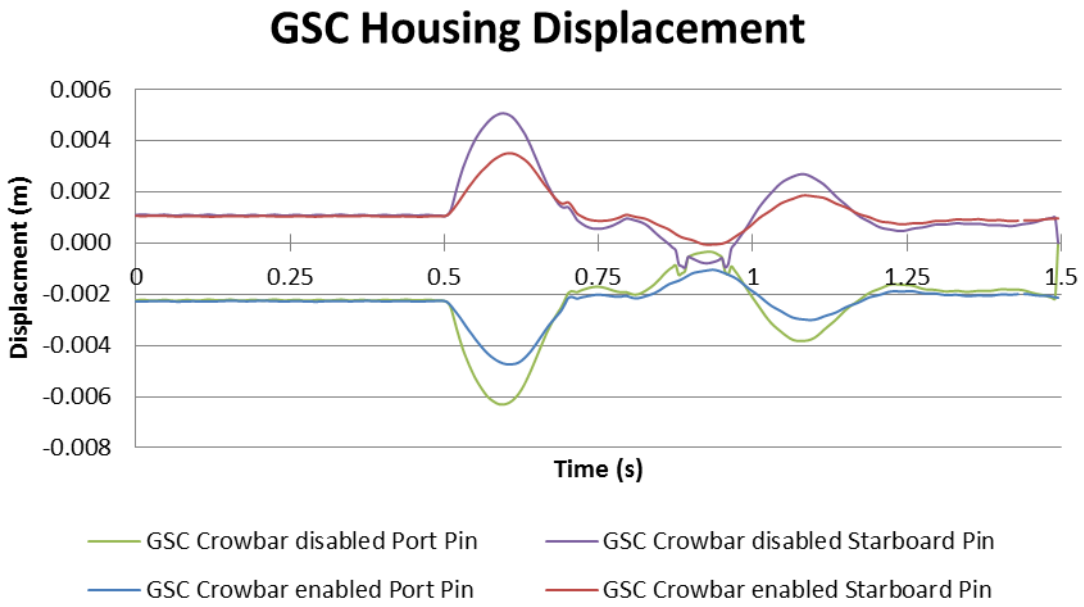

Figure 8: Housing displacement for GSC - crowbar enabled and disabled

Much like with the LSS torque and rotor speed, the enabling of the crowbar has reduced the magnitude of the gearbox housing oscillations while following the same profile. Initially a displacement of roughly 0.004m is observed followed by almost 0.006m due to the torque reversal when the crowbar is disabled. The magnitude of the oscillations then decrease to 0.004m with the final oscillation measuring roughly 0.002m, showing that the housing is settling at the end of the simulation. These results indicate that the gearbox experiences a rolling motion about the central axis

of the gearbox. It can also be seen that the effect of the crowbar is maintained throughout the simulation.

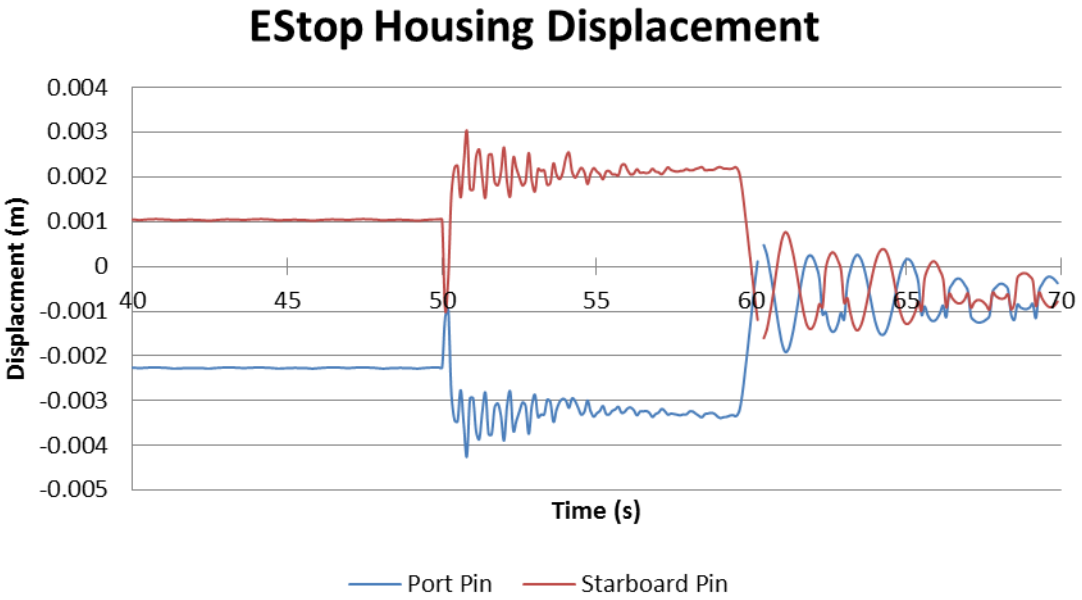

Figure 9: Housing displacement for emergency stop

On comparison with the housing displacement of the Estop simulation (Figure 9), both simulations share the initial steady state housing position. However, the magnitude of the oscillations are greater as a result of the short circuit. Although the magnitude is greater for the short circuit case its duration is significantly less than that of the Estop. As a result the potential damage caused by the displacement during the Estop case is greater. Unlike the GSC case, the Estop housing displacement does not return to the original steady state position as the turbine has been brought to a stop.

3.2. Gear Analysis

A shock load passing through a gear system has the potential to cause serious damage to gear arrangements and gear teeth. An increased load above the gears threshold can cause pitting of the gear teeth and in severe cases a fracture. In a planetary gear system, planet gears are used to not only increase the rotational speed while minimising the space required but also to split the torque load between more gears. In some cases the torque is not split evenly, known as unequal load sharing which can result in gears deteriorating at an increased rate in comparison to the others. In this analysis, focus has been aimed at the contact and bending stresses observed by the gears during the GSC. The bending and contact stress of each gear is summarised by the operational safety factor. The safety factor is defined as the ratio of the calculated maximum contact/bending stress to the maximum allowable contact stress defined in the component definition.

On a component level, it remains clear that the addition of the crowbar can mitigate the loading on the system (Figure 10). If a gear were to have a safety factor of 1, the calculated maximum stress the gear experiences is equal to that of the allowable stress it has been designed for. Figure 10 shows the worst case safety factors calculated within the duty cycle of 0.5-0.995s and it can be seen that a higher safety factor has been calculated for each of the gears when the crowbar is enabled. Gears with the lowest safety factor are contained within stage 1 of the gearbox which is the first gear stage met by the

LSS and therefore are exposed to the largest torque loads. The same is true for the bending stress safety factors shown in Figure 11

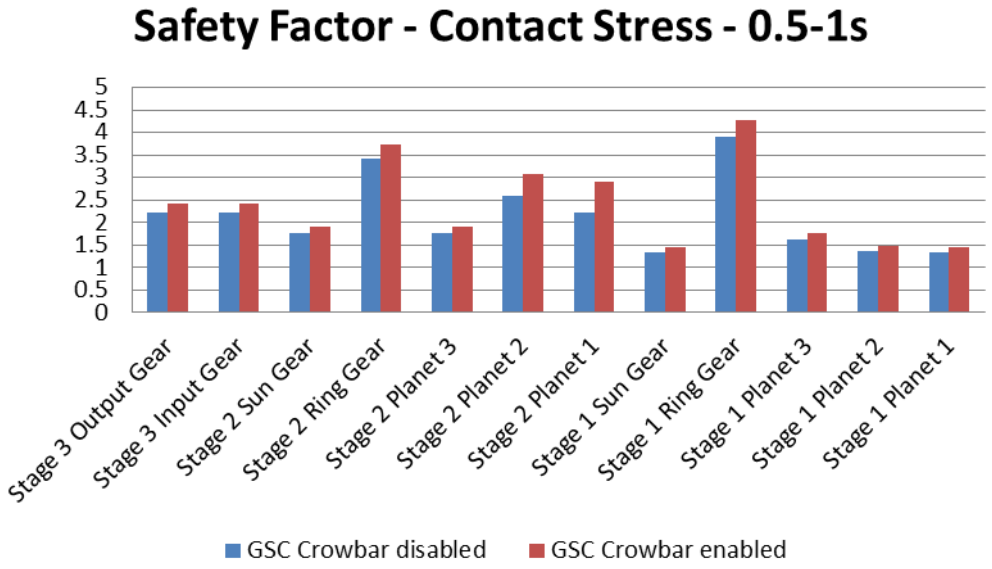

Figure 10: Contact stress safety factor for duty cycle 0.5-1.0s

In both cases the safety factor increases moving through the drivetrain as the torque decreases. The ring gears of stage 1 and stage 2 do not follow this trend regarding contact stresses. The ring gear is the only stationary gear within the gearbox and the load applied to this gear is split across the 3 planet gears. As such the contact stress applied to a gear tooth at any one time is reduced. Although the safety factor for each gear is greater than 1, the loading remains large enough to potentially reduce gear life.

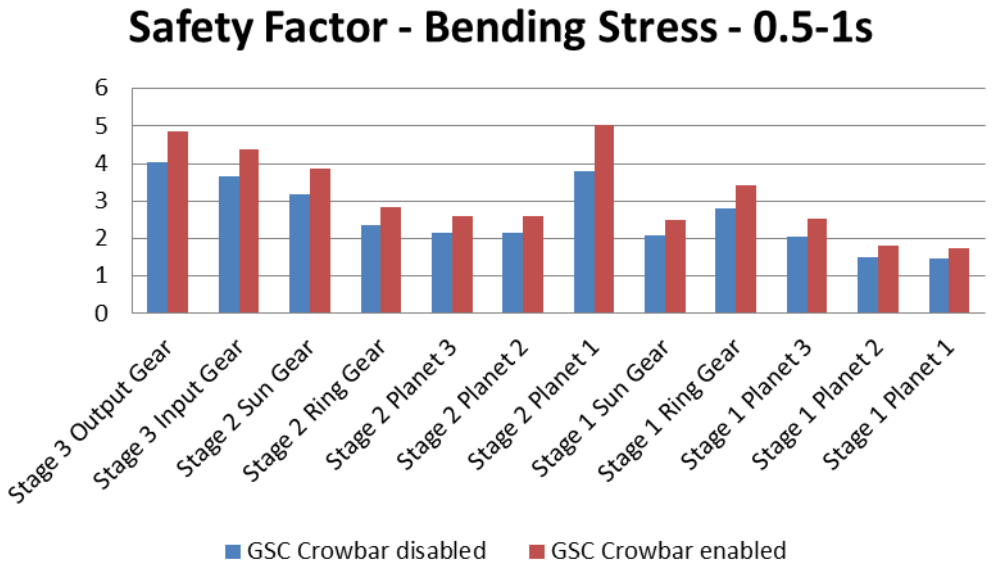

Figure 11: Bending stress safety factor for duty cycle 0.5-1.0s

On closer inspection of the stage 1 sun gear and a planet gear, the dynamics of the loading can be seen regarding the contact stresses.

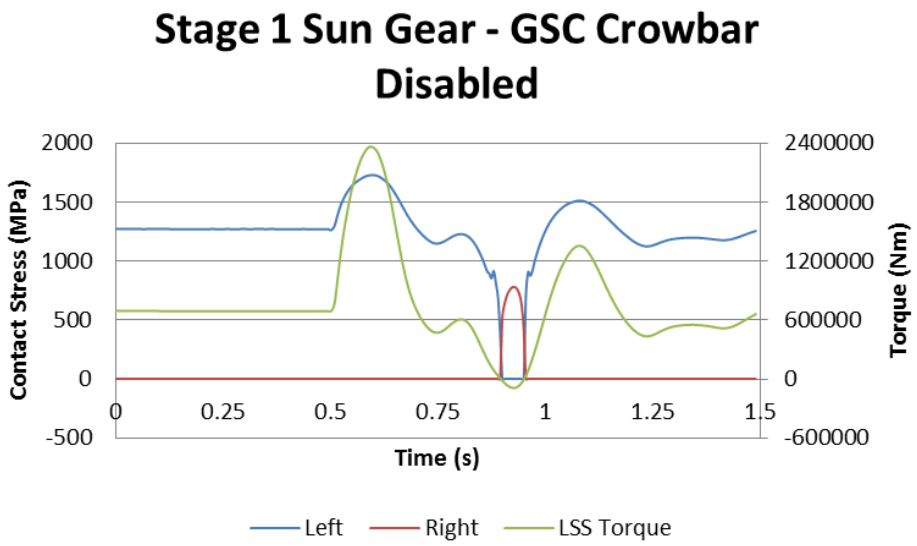

Figure 12: Stage 1 sun gear contact stress crowbar disabled

The left and right data sets refer to the flanks of the gear teeth. As the LSS torque moves from positive to negative torque, the stress applied to the gear teeth change from the initial left flank to the right flank. During steady state operation the left flank is driving the gear. Following the fault clearing, the inertia of the rotor causes a torque reversal in the LSS and the right flank becomes the driving face. To prevent unnecessary wear to gear teeth clearance is applied to the gear teeth in the form of backlash. This allows the teeth to mesh without coming into contact. When a load reversal occurs as seen in Figure 12, the gear teeth make contact. This contact is what can lead to extensive damage of the gear teeth. The planet gear also experiences this load reversal however; unlike the sun gear both flanks are experiencing various levels of contact stress throughout the simulation (Figure13).

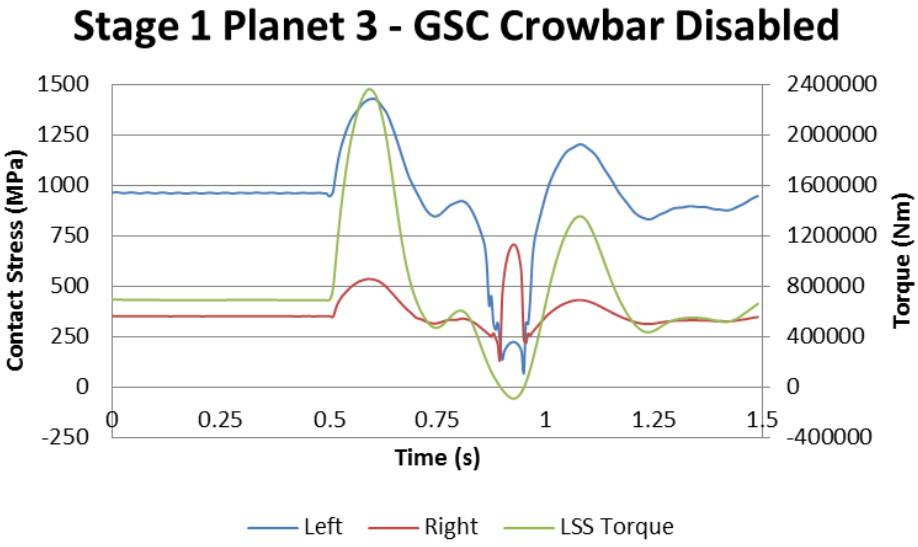

Figure 13: Stage 1 planet 3 contact stress crowbar disabled

During the planet gears operation, it is meshed with both the ring gear and the sun gear. The planet gear applies the driving force through its left flank to the left flank of the sun gear. However, the right flank of the planet gear also makes contact with the right flank of the ring gear. During the torque reversal these loads are switched and the right flank of the planet gear now makes contact with the right flank of the sun gear and subsequently the left flank makes contact with the left flank of the ring gear.

With the crowbar enabled, the torque reversal is removed and therefore the loading on the sun gear remains on the left flank as can be seen in Figure 14.

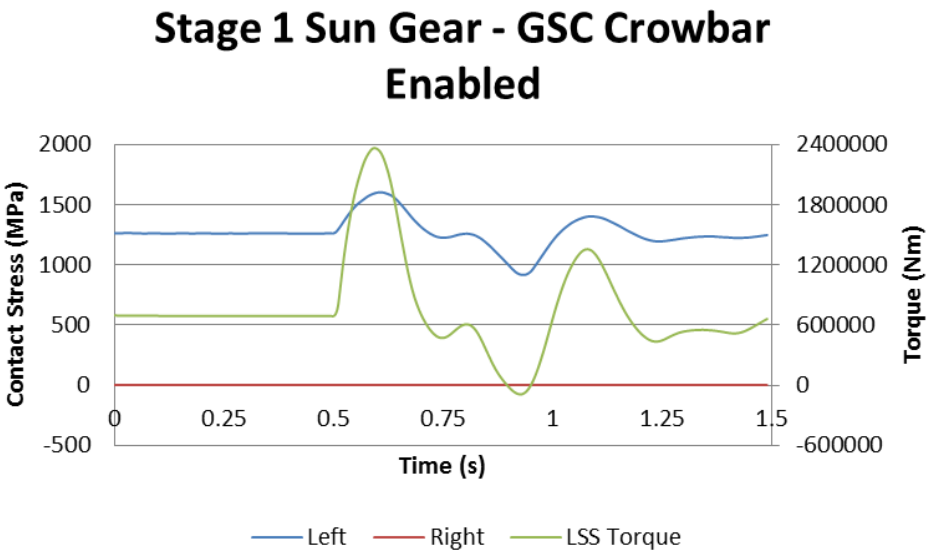

Figure 14: Stage 1 sun gear contact stress crowbar enabled

Similarly the driving load remains on the left flank of the planet gear whilst the right flank only experiences loading due to the contact with the ring gear (Figure 15).

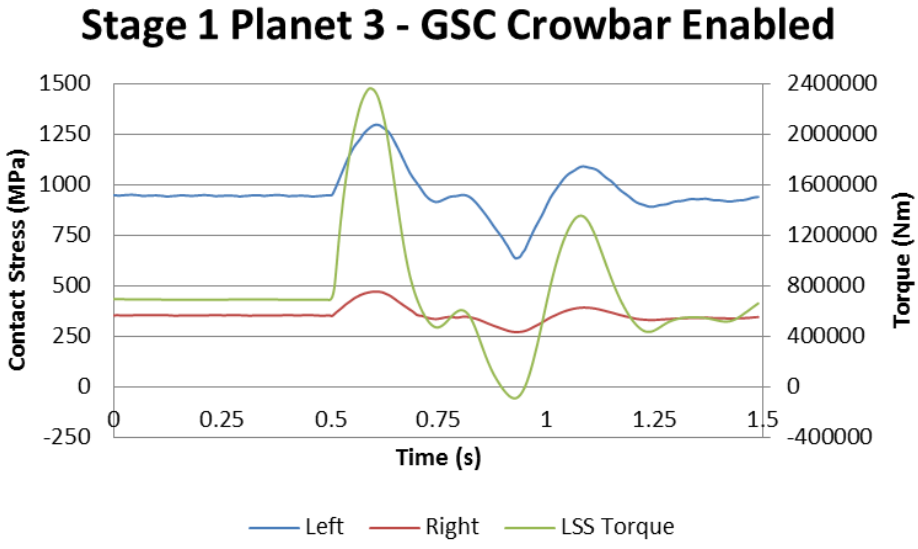

Figure 15: Stage 1 planet 3 contact stress crowbar enabled

3.3. Bearing Analysis

Testing and field data have shown that bearings are one of the major contributors to drivetrain and gearbox failure. Bearings have numerous failure modes such as skidding and pitting of the rolling elements and raceway. Shock loads to the bearings can contribute significantly to these failures, especially during load reversals. During a load reversal the load quickly shifts through 180 degrees to the unloaded rolling elements. This can cause the rolling elements to make contact with the raceway through the film of lubrication resulting in skidding, thus damaging the raceway and rolling element. misalignment of the bearings can also result in truncation where the rolling element makes contact outside of the raceway.

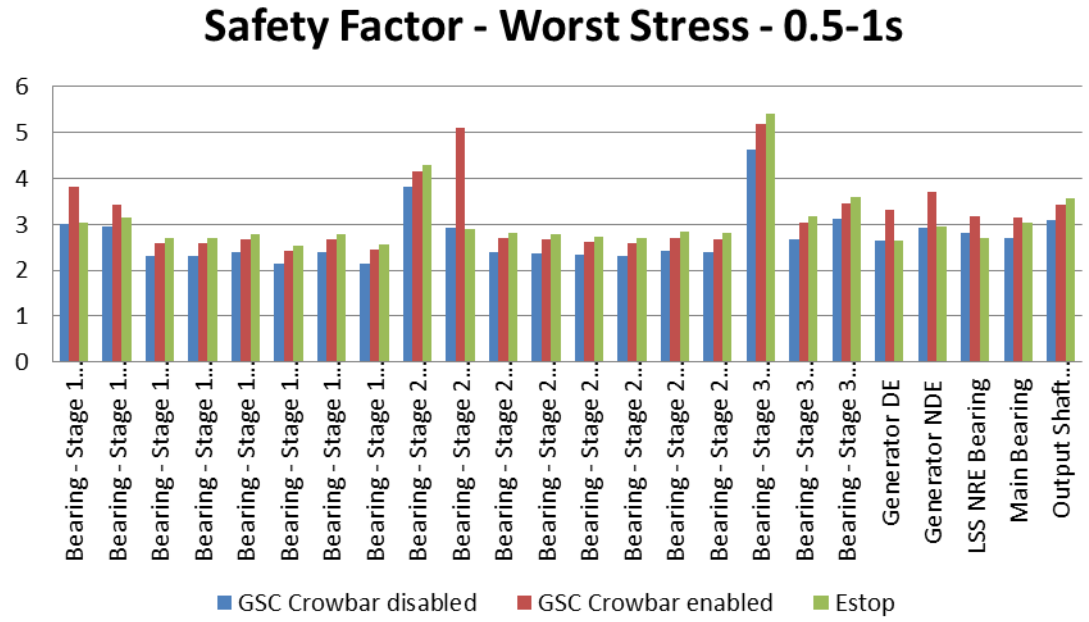

Figure 16: Worst stress safety factor for duty cycle 0.5-1.0s

Figure 16 depicts the safety factor for each bearing as a result of the worst stress experienced by this bearing. The worst stress refers to the greatest magnitude of stress exerted on the bearing during the GSC. These safety factors are well above 1, signifying that the bearings can withstand the load applied. However, this shock loading will contribute to bearing fatigue and will reduce the overall lifetime of the bearings. Figure 16 shows that each bearing shares a similar safety factor. The same can be said for the bearing safety factors under an Estop event. Literature shows that the high speed bearings are those which more commonly fail in the field.

The contact stresses experienced by the output shaft downwind bearing reflect the LSS torque profile however; when a torque reversal occurs the contact stress is applied to previously unloaded bearings. In this case the contact stress observed during the torque reversal is lower than the steady state stress.

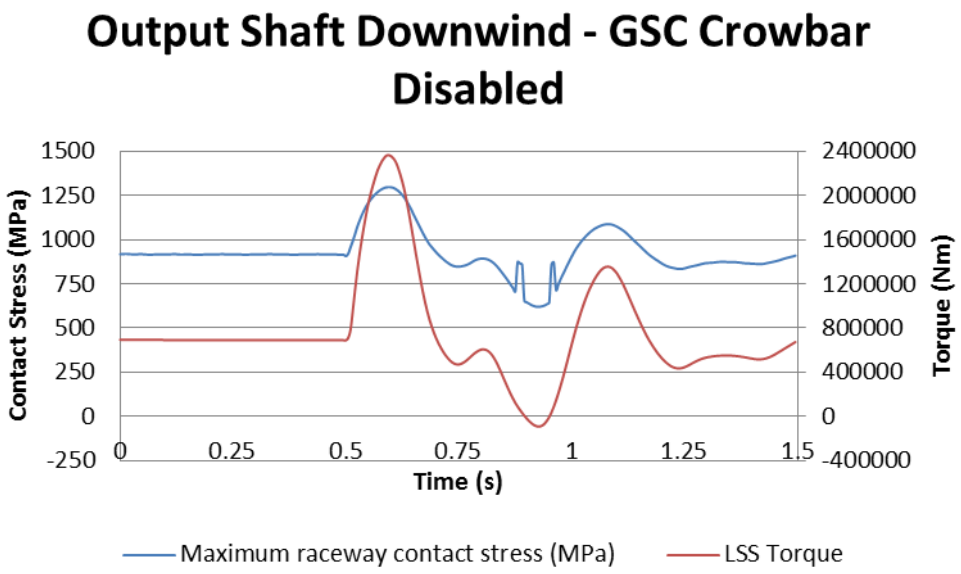

Figure 17: Output shaft downwind bearing contact stress crowbar disabled

According to literature from Romax and SKF [8], rolling elements should not experience maximum contact stresses exceeding 4GPa to prevent serious contact failure. The contact stresses generated from the GSC reach a maximum of roughly 1.3GPa. As such the bearings will be able to withstand these shock loads. When compared to the contact stresses experienced during and Estop, the maximum contact stress calculated is roughly 1.1GPa (Figure18). The maximum contact stresses also do not occur during a torque reversal and therefore are applied to already loaded bearings. The damage would be caused during the lower contact stresses with a load reversal shown after 60s in Figure 18. These stresses are also applied for a considerably longer period than those observed in the GSC.

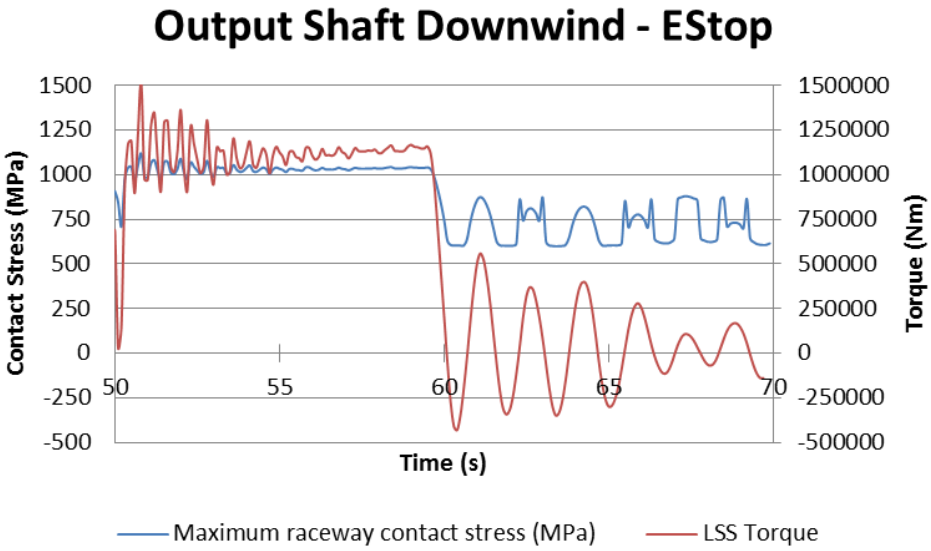

Figure 18: Output shaft downwind contact stress during Estop event

4. Conclusion

This paper has combined 3 models of varying fidelity in order to simulate wind turbine ride through following a DFIG 3 phase short circuit on the drivetrain using pseudo-static modelling methods. The analysis focused on the effects this transient event had on the drivetrain at component level as well as the level of loading mitigation provided by the use of crowbar protection. Following a short circuit event, the gearbox housing displacement was greater than that of a simulated emergency stop although for a much shorter period. Analysis on the gears and bearings showed signs of load reversal without the assistance of crowbar protection however, the safety factors calculated for all components showed that these shock loads were well within their operating thresholds. It is believed that although these loads are not of a magnitude which could directly cause a component to fail, they could significantly contribute to reducing the lifetime of the component depending on the frequency of the events. This will be the subject of future study and analysis.

Acknowledgements:
This work has been carried out with the support of Romax Technology and has been funded by the EPSRC, project reference number EP/G037728/1. The author would also like to acknowledge assistance from Dr Alasdair McDonald, University of Strathclyde.

References

[1] F. Spinato, P. J. Tavner, G. J. W. van Bussel, and E. Koutoulakos, "Reliability of wind turbine subassemblies," *IET Renew. Power Gener.*, vol. 3, no. 4, p. 387, Dec. 2009.

[2] S. Sheng, "Report on Wind Turbine Subsystem Reliability-A Survey of Various Databases," 2013.

[3] J. Morren and S. W. H. de Haan, "Short-Circuit Current of Wind Turbines With Doubly Fed Induction Generator," *IEEE Trans. Energy Convers.*, vol. 22, no. 1, pp. 174–180, 2007.

[4] J. Ouyang and X. Xiong, "Research on short-circuit current of doubly fed induction generator under non-deep voltage drop," *Electr. Power Syst. Res.*, vol. 107, pp. 158–166, 2014.

[5] F. Sulla, J. Svensson, and O. Samuelsson, "Short-circuit analysis of a doubly fed induction generator wind turbine with direct current chopper protection," *Wind Energy*, vol. 16, no. 1, pp. 37–49, 2013.

[6] A. Johnson, "Grid Code Workshop Fault Ride Through – Background," 2013.

[7] K. Scott, "Effects of Transient Loading on Wind Turbine Drivetrains," University of Strathclyde, 2014.

[8] SKF, "SKF rating life." [Online]. Available: http://www.skf.com/group/products/bearings-units-housings/roller-bearings/principles/selection-of-bearing-size/selecting-bearing-size-using-the-life-equations/skf-rating-life/index.html. [Accessed: 28-Sep-2014].